2. REPORT DATE: December 1, 1992

3. REPORT TYPE AND DATES COVERED: Reprint

4. TITLE AND SUBTITLE
Temperature, Kinetic Energy, and Rotational Temperature Effects in Four Reactions Involving Isotopes

5. FUNDING NUMBERS
PE 61102F
PR 2303
TA G5
WU 01

6. AUTHOR(S)
A.A. Viggiano, Robert A. Morris, Jane M. Van Doren, John F. Paulson, H.H. Michels*, R.H. Hobbs*, Christopher E. Dateo**

7. PERFORMING ORGANIZATION NAME(S) AND ADDRESS(ES)
Phillips Lab/GPID
Hanscom AFB
Massachusetts 01731-5000

8. PERFORMING ORGANIZATION REPORT NUMBER
PL-TR-92-2316

9. SPONSORING/MONITORING AGENCY NAME(S) AND ADDRESS(ES)

10. SPONSORING/MONITORING AGENCY REPORT NUMBER

11. SUPPLEMENTARY NOTES
*United Technologies Research Center, East Hartford, CT 06108
**Department of Chemistry, University of California, Santa Barbara, CA 93106
Reprinted from Isotope Effects in Gas-Phase Chemistry, Chapter 15, 1992 American Chemical Society

12a. DISTRIBUTION/AVAILABILITY STATEMENT
Approved for public release; Distribution unlimited

12b. DISTRIBUTION CODE

13. ABSTRACT (Maximum 200 words)
Data on four reactions involving isotopes taken in a variable temperature-selected ion flow drift tube are presented. A study of the reaction of O^- with N_2O indicates that the reaction proceeds preferentially by bonding of the O^- to the central nitrogen in N_2O. The preference for O^- attack at the central nitrogen over attack at the terminal nitrogen decreases at higher temperatures. In the atom abstraction reaction of O^+ with HD, OH^+ is formed more efficiently than is OD^+ at low temperatures and moderate energy. The branching fraction favoring OH^+ production is also sensitive to the rotational temperature of the HD. The results for this reaction are consistent with a model of the reaction based on the long range part of the ion-neutral potential. Rate constants for the reactions of O^- with H_2, D_2, and HD vary with mass of the hydrogen molecule as predicted from the collision rate constant dependence. These reactions proceed by two channels: hydrogen abstraction and associative electron detachment. The rate constant for the minor hydrogen abstraction channel increases with increasing kinetic energy. The efficiency of the abstraction reaction of O^- with D_2 is significantly smaller than that in the reaction with H_2. More OD^- as compared with OH^- is produced in the reaction of HD. The results are explained by a direct two step mechanism. A large preference for OH^- over OD^- formation in the atom abstraction reaction of O^- with CH_2D_2 is observed. An *ab initio* potential for the reaction path reveals a barrier and indicates that zero point energy effects play a major role in the observed isotope effects. The four reactions studied in this paper, when taken together, show that isotopically labelled reactants can be important in elucidating widely different reaction mechanisms.

14. SUBJECT TERMS
Rate constants, Branching ratios, Isotopes

15. NUMBER OF PAGES
21

16. PRICE CODE

17. SECURITY CLASSIFICATION OF REPORT	18. SECURITY CLASSIFICATION OF THIS PAGE	19. SECURITY CLASSIFICATION OF ABSTRACT	20. LIMITATION OF ABSTRACT
Unclassified	Unclassified	Unclassified	SAR

PL-TR-92-2316

Chapter 15

Temperature, Kinetic Energy, and Rotational Temperature Effects in Four Reactions Involving Isotopes

A. A. Viggiano[1], Robert A. Morris[1], Jane M. van Doren[1], John F. Paulson[1], H. H. Michels[2], R. H. Hobbs[2], and Christopher E. Dateo[3]

[1]Phillips Laboratory, Geophysics Directorate, Ionospheric Effects Division (LID), Hanscom Air Force Base, MA 01731–5000
[2]United Technologies Research Center, East Hartford, CT 06108
[3]Department of Chemistry, University of California, Santa Barbara, CA 93106

Data on four reactions involving isotopes taken in a variable temperature-selected ion flow drift tube are presented. A study of the reaction of O^- with N_2O indicates that the reaction proceeds preferentially by bonding of the O^- to the central nitrogen in N_2O. The preference for O^- attack at the central nitrogen over attack at the terminal nitrogen decreases at higher temperatures. In the atom abstraction reaction of O^+ with HD, OH^+ is formed more efficiently than is OD^+ at low temperatures and moderate energy. The branching fraction favoring OH^+ production is also sensitive to the rotational temperature of the HD. The results for this reaction are consistent with a model of the reaction based on the long range part of the ion-neutral potential. Rate constants for the reactions of O^- with H_2, D_2, and HD vary with mass of the hydrogen molecule as predicted from the collision rate constant dependence. These reactions proceed by two channels: hydrogen abstraction and associative electron detachment. The rate constant for the minor hydrogen abstraction channel increases with increasing kinetic energy. The efficiency of the abstraction reaction of O^- with D_2 is significantly smaller than that in the reaction with H_2. More OD^- as compared with OH^- is produced in the reaction of HD. The results are explained by a direct two step mechanism. A large preference for OH^- over OD^- formation in the atom abstraction reaction of O^- with CH_2D_2 is observed. An *ab initio* potential for the reaction path reveals a barrier and indicates that zero point energy effects play a major role in the observed isotope effects. The four reactions studied in this paper, when taken together, show that isotopically labelled reactants can be important in elucidating widely different reaction mechanisms.

NOTE: The Phillips Laboratory was formerly the Air Force Geophysics Laboratory.

0097–6156/92/0502–0225$06.25/0

Studies involving isotopically labeled reactants can yield important insights into reaction mechanisms. In particular, the extent of isotope incorporation into the products formed can shed light on the structure of the prinicipal complex(es)/ intermediate(s) involved in the reaction. In addition, kinetic isotope effects may provide insight into the reaction mechanism by providing information about the reaction coordinate potential energy curve. Frequently, large kinetic isotope effects are seen only in reactions involving hydrogen and deuterium. However, several examples in this volume show that significant kinetic isotope effects can occur in reactions involving heavier isotopes. The temperature, kinetic energy, and rotational energy dependence of the rate constant and branching ratios can provide further information on the reaction coordinate potential and mechanism.

The selected ion flow tube is a versatile system for studying reactions involving isotopes. The reactant ion is formed in a remote ion source, mass selected, and injected into the reaction flow tube. This "sifting" prevents the neutral precursor of the reactant ion from entering the reaction region and eliminates unwanted isotopic mixtures of the reactant ion at different masses. Many isotopically labeled reactions have been studied using such systems.[1] In addition to these advantages, the present selected ion flow tube can be heated or cooled over a wide range, and the kinetic energy of the reactant ions can be varied by application of a drift field.[2] This apparatus is designated VT-SIFDT for variable temperature-selected ion flow drift tube. From studies of rate constants or branching ratios as a function of kinetic energy at several temperatures, information on the influences of rotational and vibrational energy on a variety of reactions can be obtained.[2-5]

In this paper we report results on four reactions involving isotopically labeled reagents. The goal in all of these studies was to elucidate the reaction mechanism. An important aspect of these studies was the variation of the isotopic effects with temperature, kinetic energy, and rotational energy.

Experimental

The measurements were made using the Phillips Laboratory (formerly the Geophysics Laboratory) variable temperature-selected ion flow drift tube apparatus.[2] Instruments of this type have been the subject of review,[6] and only those aspects important to the present study will be discussed in detail. Ions are created by electron impact in a moderate pressure ion source (~ 0.1 torr). The ions are extracted from the source and mass selected in a quadrupole mass filter. Ions of the desired mass are injected into a meter-long flow tube through a small orifice, 2 mm in diameter. A buffer gas, helium unless otherwise noted, transports the ions along the length of the flow tube. The pressure in the flow tube is ~0.5 torr. The buffer gas is added through a Venturi inlet surrounding the ion injection orifice and thus aids in injecting the ions at low energy. A drift tube, consisting of 60 electrically insulated rings connected by resistors, is positioned inside the flow tube. A voltage can be applied to the resistance chain in order to produce a uniform electric field inside the flow tube for studies of energy dependence. The bulk of the gas in the flow tube is pumped by a Roots type blower. The flow tube is terminated by a truncated nose cone. A small fraction of the ions in the flow tube is sampled through a 0.2 mm hole in the nose cone, mass analyzed in a second quadrupole mass spectrometer, and detected by a channel electron multiplier.

Neutral reactant gas is added through one of two inlets. The inlets are rings with a series of holes pointing upstream.[2] The area inside the ring is equal to the area between the ring and the tube wall to aid in quickly distributing the reactant gas

throughout the cross sectional area of the flow tube. Rate constants are measured by monitoring the decay of the primary ion signal as a function of added neutral flow. This is done at each of the two neutral inlets, and an end correction is determined from those data. Ion flight times are measured by applying an electrical retarding pulse to two of the drift tube rings consecutively and measuring the two arrival time spectra of the ions. The ion velocity and therefore the reaction time are determined from these data and from knowledge of the relevant distances. Pressure is monitored by a capacitance manometer. Flow rates of the buffer and of the reactant gas are controlled and measured by MKS flow controllers. The rate constant is determined, using data obtained at each inlet, from the slope of the line obtained by plotting the logarithm of the reactant ion signal decay versus neutral reactant flow, and from the values of the pressure, temperature, flow rates of the reactant and buffer, and ion velocity. The final rate constant incorporates the end correction. The entire flow tube can be heated or cooled over the range 85 to 550 K.

Branching fractions are measured by monitoring the signals from the ionic products and determining the fraction of the total products that each product represents at each neutral flow rate. These fractions are plotted versus neutral flow rate, and the resulting curves are extrapolated to zero neutral flow to account for secondary reactions. The branching fractions reported are the extrapolated values. No correction for mass discrimination was made in the studies reported here because the different product ions in each reaction have very small mass differences.

The average kinetic energy in the ion-neutral center-of-mass system, $\langle KE_{cm} \rangle$, in the drift tube is derived from the Wannier formula[7] as

$$\langle KE_{cm} \rangle = \frac{(m_i + m_b)m_n}{2(m_i + m_n)} v_d^2 + \frac{3}{2} kT \qquad (1)$$

where m_i, m_b, and m_n are the masses of the reactant ion, buffer gas, and reactant neutral, respectively; v_d is the ion drift velocity; and T is the temperature. The first term in the formula is the energy supplied by the drift field, and the second term is the thermal energy. This formula is an excellent approximation of the ion energy at low ion energies.[8,9] At energies approaching 1 eV the formula is still good to within ±10%. The neutral reactant temperature under the conditions of the present experiments is the same as that of the buffer gas since the neutral gas enters the flow tube through inlets at the same temperature as the flow tube and suffers many collisions with the walls of the inlets before entering the flow tube. The ions used in the present studies are all monatomic, and therefore the drift tube can influence only the ion translational energy (no electronic excitation is expected for the drift tube energies employed here). The distribution of ion energies in a helium buffer is very nearly Maxwellian at an effective temperature, T_{eff}, such that $\langle KE_{cm} \rangle = 3/2kT_{eff}$.[8-11] By "nearly Maxwellian", it is meant that the distribution of ion energies is such that the rate constant measured in the drift tube is indistinguishable from that which would be measured for a Maxwellian distribution (within the 15% experimental precision).

It has recently been shown in our laboratory that dependences of rate constants or branching ratios on the internal temperature of the reactant neutrals can be derived for a variety of ion-molecule reactions by measuring rate constants or branching ratios as a function of $\langle KE_{cm} \rangle$ at several temperatures.[2-5,9,12,13] If the ions are monatomic, as in the present studies, comparing the rate constants or branching ratios at a particular $\langle KE_{cm} \rangle$ but at different temperatures yields the

dependence of the rate constant on the internal temperature of the reactant neutral. If the neutral has no low frequency vibrational modes, this dependence is a rotational temperature dependence.

O^+ was formed from CO by dissociative electron impact ionization. This source produced 98% of the O^+ ions in the ground ^4S state. The fraction of excited state O^+ was monitored by allowing the O^+ ions to react with CO in the flow tube. CO reacts with the excited metastable states of O^+ and does not react with the ground state.[1] CO_2 and O_2 were tested as alternative sources of O^+ but produced more metastable ions. The 2% fraction of O^+ in the excited state remained constant over the course of these experiments. $^{16}O^-$ was generated by dissociative electron attachment to N_2O, while $^{18}O^-$ was generated by dissociative attachment to $^{18}O_2$.

All reactant gases were obtained commercially and used without further purification. The HD was ≥98.7% isotopically pure, and no corrections for incomplete labeling were made to the data. According to the manufacturers the HD may be purer than this but the absolute purity could not be measured with greater accuracy. The $^{14}N^{15}NO$ was of 99% isotopic purity, and the product distributions were corrected for the slight $^{14}N_2O$ impurity. The CH_2D_2 was 98% isotopically pure, and no corrections to the data were made since it is not certain which isotopic form of CH_4 the impurities are.

The rate constant for the reaction of O^- with unlabeled N_2O was measured in a helium buffer as a function of $\langle KE_{cm} \rangle$ at several temperatures. The reactions with labeled N_2O were studied in an argon buffer. For the reaction of the unlabeled species we were interested in the dependence of the rate constant only on the internal temperature of N_2O. This required the use of a helium buffer so that the distribution of kinetic energies at a particular $\langle KE_{cm} \rangle$ would be essentially Maxwellian and thus approximately independent of temperature.[8-11] The goal of the isotopic labeling studies of N_2O was to determine the reaction mechanism by monitoring the distribution of isotopes in the NO^- products. This required an argon buffer so that no detachment of the NO^- product ions would occur. Helium is known to detach the weakly bonded electron[14] from NO^-, but the electron remains attached to NO^- in an argon buffer.[12] In argon, the product ion signals balanced the loss of primary ion signal, indicating that electron detachment from the product ions was minimal. The requirement of an argon buffer (and the cost of $^{14}N^{15}NO$) prevented us from studying the reaction of the completely labeled reactants using the drift tube because the ion kinetic energy distributions produced in an argon buffer are known to be non-Maxwellian.[11,15,16] Such non-Maxwellian distributions would confuse any attempt to derive internal temperature dependences in the branching fraction for the labeled systems.

O^+ reacts with water to produce H_2O^+. This ion has the same mass as that of the OD^+ product ion in the reaction of O^+ with HD. Since we expected small effects on the branching ratio of this reaction, the flow tube had to be essentially free of water vapor. In order to accomplish this goal several steps were taken. Ultra high purity helium was used (99.9999%) and passed through a molecular sieve trap cooled to liquid nitrogen temperature. The flow tube was repeatedly baked at 550 K over the course of several weeks, and the helium inlets were also heated over the same time frame. The system was not exposed to air during the course of this baking. The baking reduced the amount of conversion of O^+ to H_2O^+ at 300 K from over 20% at the start of the process to an undetectable amount. The maximum water vapor concentration in the flow tube is estimated to be 10^8 cm^{-3}, or a mixing ratio of

~10^{-8}. At 509 K, about 1% of the O^+ was converted to H_2O^+. The branching fractions observed were corrected for this small mass 18 impurity. The water impurity at 509 K leads to an uncertainty of 2.5 percentage points in the branching fractions (expressed as percentages) derived at 509 K. The uncertainty at other temperatures is 1.5 percentage points. All of the branching fraction data were extrapolated to zero HD flow rate since OH^+ and OD^+ react with HD to form various H_2O^+ isotopomers which further react to form H_3O^+ in all of the isomeric forms. Reactions involving OH^- and OD^- products were simpler since no secondary reactions occurred under the conditions of our experiments.[17]

Results and Discussion

a) The Reaction of O^- With N_2O. The reaction of unlabeled reactants produces NO^- and NO,

$$O^- + N_2O \rightarrow NO^- + NO. \quad (2)$$

The reaction is exothermic by 0.14 eV.[18] The goal of using isotopically labeled reagents to study this reaction was to determine the fraction of interactions in which the O^- attacks the central nitrogen versus the terminal nitrogen in N_2O. Our results for this reaction, for both labeled and unlabeled reactants, have been published previously[19] and will be summarized below.

The rate constant for this reaction was studied at four temperatures over the range 143 K to 515 K.[19] The rate constant was found to decrease with increasing temperature or energy from a value of 2.9 x 10^{-10} cm^3 s^{-1} at 143 K (0.019 eV) to a minimum of 8-9 x 10^{-11} cm^3 s^{-1} at approximately 0.5 eV. Above 0.5 eV, the rate constant increases to a value of 1.1 x 10^{-10} cm^3 s^{-1} at 0.92 eV. However, at a particular kinetic energy, no temperature dependence of the rate constant was found. This implies that there is no dependence on the internal temperature of the N_2O over this temperature range, indicating that neither rotational energy nor excitation of the N_2O bending mode, the lowest energy vibrational mode, has a large effect on reactivity between 143 and 515 K.

Several aspects of the reaction have been investigated using isotopic labeling. Van Doren *et al.*[20] have shown that the oxygen atoms exchange with a rate constant of 1.7 x 10^{-10} cm^3 s^{-1},

$$^{18}O^- + N_2{}^{16}O \rightarrow {}^{16}O^- + N_2{}^{18}O. \quad (3)$$

The same oxygen exchange rate was measured for the reaction of totally labeled reactants, i.e., labeling of both nitrogen and oxygen.[19,21] At 143 K, the rate constant for O^- exchange was found to be 1.4 x 10^{-10} cm^3 s^{-1}, indicating that the rate constant for this channel has a small positive temperature dependence. Interestingly, the efficiency for the sum of the two channels, reactions 2 and 3, is approximately temperature independent over this temperature range. Therefore, as the efficiency for NO^- production decreases with increasing temperature, the efficiency for O^- exchange appears to increase by the same amount. The positive temperature dependence for oxygen exchange may result from a small activation energy (presumably from the breaking of the O - N_2 bond). Alternatively, it may be due to

the fact that the contribution from the reactive channel producing NO^- decreases, leaving a larger fraction of "unreactive collisions" which can result in O^- exchange.

In one set of experiments, we studied this reaction using unlabeled oxygen and labeled nitrogen.[19]

$$O^- + {}^{14}N{}^{15}NO \rightarrow {}^{14}NO^- + {}^{15}NO \qquad (4)$$
$$\rightarrow {}^{15}NO^- + {}^{14}NO.$$

In that study, we observed equal production of $^{14}NO^-$ and $^{15}NO^-$ at both 143 K and 298 K. This is consistent with the findings of Barlow and Bierbaum.[21] At higher energies (about 1 eV), Paulson[22] found that there was a preference for the O^- to pick up the terminal nitrogen in the ratio of 1.25:1. This suggests that at higher energies there may be a change in the mechanism from one involving a long lived complex/intermediate to a direct process such as atom stripping. The involvement of a direct mechanism at high energy could explain the increase in the rate constant at energies above 0.5 eV and the change in the energy dependence of the rate constant from negative to positive.

We have also studied the reaction using both labeled nitrogen and oxygen atoms,

$$^{18}O^- + {}^{14}N{}^{15}N{}^{16}O \rightarrow {}^{14}N{}^{16}O^- + {}^{15}N{}^{18}O \qquad (5)$$
$$\rightarrow {}^{15}N{}^{16}O^- + {}^{14}N{}^{18}O$$
$$\rightarrow {}^{14}N{}^{18}O^- + {}^{15}N{}^{16}O$$
$$\rightarrow {}^{15}N{}^{18}O^- + {}^{14}N{}^{16}O$$
$$\rightarrow {}^{16}O^- + {}^{14}N{}^{15}N{}^{18}O.$$

Figure 1 shows a plot of the percentage of the total NO^- production contributed by each of the four possible NO^- isotopic products as a function of temperature. The data sort themselves into two groups. Masses 30 and 33 are produced on the order of 15% each and masses 31 and 32 on the order of 35% each. This is again consistent with the findings of Barlow and Bierbaum.[21] Increasing temperature leads to decreases in the percentages of masses 30 and 33, and increases in the percentages of masses 31 and 32. The negative temperature dependence of mass 33 and the positive dependence of the mass 32 are outside our estimated uncertainty. The uncertainies in the fractions of masses 30 and 31 are larger due to secondary chemistry and the temperature dependences are within the uncertainty. However, it is expected that the fractions of masses 30 and 33 are equal, as are those of masses 31 and 32. The apparent difference in the dependences of masses 31 and 32 probably results in the uncertainty in determining the fraction of mass 31 which is affected by secondary chemistry.

As stated previously, the main goal of the labeling studies was to determine whether the reaction producing NO^- proceeds by O^- reaction at the central or terminal nitrogen. If the reaction were to proceed exclusively by terminal attack without migration of O^-, one would expect equal abundances of masses 31 and 32 with no production of masses 30 and 33. This expectation assumes that it is equally probable that the charge remains on either NO fragment. This assumption is supported by the data obtained using labeled nitrogen and unlabeled oxygen, reaction 4, where equal fractions of the two possible NO^- products were observed. Attack exclusively at the central nitrogen should produce all four isotopically labeled NO^- species with equal

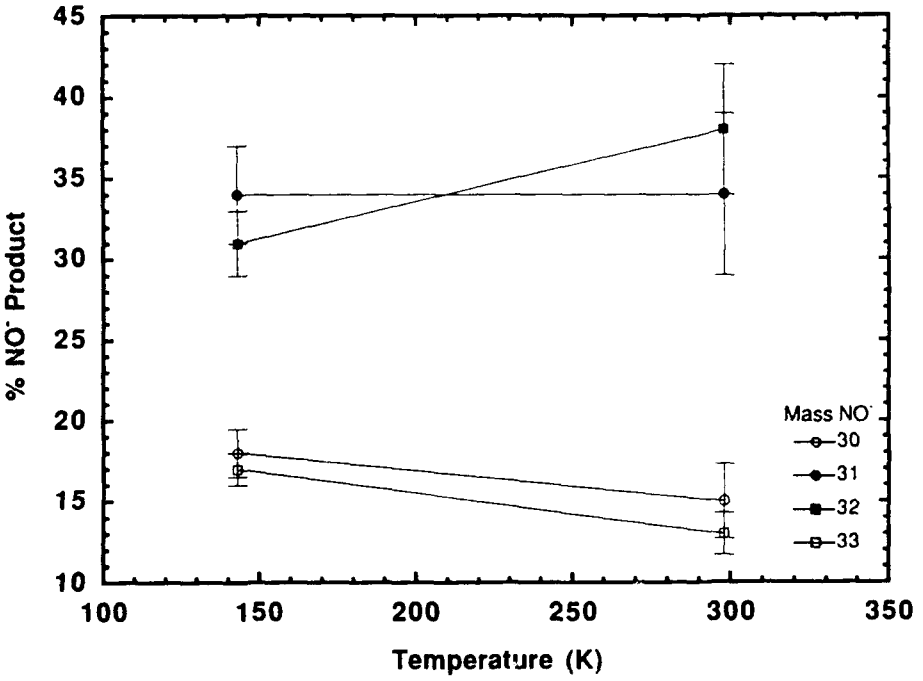

Figure 1. Percent contribution to the total NO^- production by the individual NO^- isotopes in the reaction of $^{18}O^-$ with $^{14}N^{15}N^{16}O$ as a function of temperature. Open circles, solid circles, solid squares, and open squares represent $^{14}N^{16}O^-$, $^{15}N^{16}O^-$, $^{14}N^{18}O^-$, and $^{15}N^{18}O^-$, respectively.

probability since the stable form of the complex formed by central attack is of C_{2v} symmetry.[23-25]

Assuming the above probabilities for forming the various isotopically labeled NO^- products for the two positions of attack on N_2O by O^-, we can derive the fractions of the reaction that proceed through reaction at the central and terminal nitrogen. The fraction of the total NO^- produced that originates from the central nitrogen is twice the sum of the mass 30 and 33 fractions, which are equal within experimental uncertainty. Thus we find that in 70% of the reactive collisions at 143 K the O^- reactant bonds to the central nitrogen. At 298 K, bonding to the central nitrogen proceeds in 56% of the reactive collisions. Multiplying these fractions by the rate constants for the reaction of the unlabeled reactants, reaction 2, yields rate constants of 2.0×10^{-10} cm^3 s^{-1} at 143 K and 1.1×10^{-10} cm^3 s^{-1} at 298 K for reaction at the central nitrogen. The rate constants for the unlabeled reagents are used since they are known the most accurately. Within our experimental uncertainty isotopic substitution does not change the rate constant for production of NO^-, i.e., there is no kinetic isotope effect in this reaction, as expected.[19] Using the same procedure, we find the rate constants for reaction at the terminal nitrogen to be 0.9×10^{-10} cm^3 s^{-1} at both temperatures. The rate constant for the central nitrogen reaction channel has a negative temperature dependence of $T^{-0.8}$, while the rate constant for the terminal nitrogen channel is independent of temperature. The negative temperature dependence of the reaction rate constant for NO^- formation, reaction 2, between 143 and 298 K arises from the temperature dependence of the reaction at the central nitrogen.

The difference in the temperature dependences of these two reactive channels forming NO^- may arise from increased rotational energy of the reactant N_2O with increasing temperature. As the molecule rotates faster it is harder for the O^- to approach the central nitrogen before encountering one of the end atoms. This increases the relative number of encounters in which the O^- hits the terminal nitrogen on first approach. Alternatively, the reaction may be initiated by terminal attack followed by migration of one of the O atoms to the central nitrogen. Increasing temperature would decrease the amount of migration, either through a decrease in the complex lifetime or because the migration involves a tight transition state which is known to lead to a negative temperature dependence.[26-28] Other mechanisms are also conceivable, and an answer to the exact nature of the competition between central and terminal attack awaits detailed calculations.

The fact that more than half of the reactive collisions proceed via reaction of the O^- at the central nitrogen is probably a result of the central nitrogen having a partial positive charge, while the terminal nitrogen is approximately neutral.[29] In spite of this, the abundance of reaction at the central nitrogen was surprising since it has been demonstrated that most reactions of anions with N_2O appear to proceed via reaction of the anion at the terminal nitrogen in N_2O.[30,31] The difference between the reaction of O^- with N_2O and the other systems studied may simply be due to steric factors. O^- is a small negative ion that can easily approach the central nitrogen. The other anions studied in reaction with N_2O are molecular, and the approach to the central nitrogen may be sterically hindered.

b) The Reaction of O^+ with HD. The reaction of O^+ with HD proceeds by hydrogen abstraction.

$$\begin{aligned} O^+ + HD &\rightarrow OH^+ + D \\ &\rightarrow OD^+ + H. \end{aligned} \qquad (6)$$

The reaction is exothermic by approximately 0.5 eV.[18] We have measured the rate constant and product branching fractions as a function of $\langle KE_{cm} \rangle$ at temperatures of 93, 300, and 509 K. The rate constant was found to be 1.2×10^{-9} cm^3 s^{-1} independent of temperature or energy within a rather large experimental uncertainty (±40%). The large uncertainty results from taking only one set of data at each inlet port, resulting in a larger than normal error in the end correction. In addition each run included recording of the signals from the ionic products in order to determine the branching fractions. The consequent increased data collection time results in greater scatter in the rate constant data due to drift in the reactant ion signal over time. More runs were not taken due to the cost of HD and the fact that our interest was mainly in the branching ratio, which does not depend on the end correction.

In Figure 2, the fraction of OH^+ produced in the reaction is plotted as a function of $\langle KE_{cm} \rangle$. Circles, squares and diamonds represent data taken at 93, 300, and 509 K, respectively. At each temperature, the fraction of OH^+ increases with increasing kinetic energy. At a particular $\langle KE_{cm} \rangle$, the OH^+ fraction decreases with increasing temperature. The difference between the fractions measured at 93 K and 300 K is larger than that between 300 K and 509 K. The latter difference for each point is smaller than our estimated error limits. The difference is probably real since every 509 K point is lower than the corresponding 300 K point at the same $\langle KE_{cm} \rangle$ and the error limits refer mostly to random error. A difference between 300 K and 509 K is also consistent with a difference between 93 and 300 K. As explained in the experimental section, the observation of different values for the branching fraction at the same $\langle KE_{cm} \rangle$ but different temperatures indicates that the branching fraction depends on the rotational temperature of the HD. Our observations indicate that kinetic and rotational energy have opposite effects on the branching fraction.

The observed energy dependences for this reaction are explained theoretically by the work of Dateo and Clary,[32] who assumed that the reactivity (both rate constant and branching fraction) is dominated by the long range part of the potential. This assumption seems justified in the present case because the reaction is very exothermic, proceeds on every collision, and has no competing channels. The form of the potential assumed by Dateo and Clary is

$$V(R,\theta) = -\frac{q\alpha}{2R^4} + q^2\left(\frac{\Theta}{R^3} - \frac{\alpha_2}{2R^4}\right)P_2\cos(\theta) \qquad (7)$$

where q is the ionic charge, α is the polarizability of HD, R is the length of a line L connecting the center of the O^+ ion to the center-of-mass of the HD, θ is the angle between the line L and the HD bond axis, Θ is the quadrupole moment of HD, and α_2 is the anisotropic polarizability of HD. The potential is the sum of the ion-induced dipole potential term, the ion-quadrupole potential term, and a term that allows the polarizability to be anisotropic. This potential was used in a rotationally adiabatic capture theory. The rate constant calculated using this theory is determined by the rate of passage over the centrifugal barrier, while the branching fraction is determined by the end of the HD molecule which points at the O^+ at the centrifugal barrier. Dateo and Clary assumed that the reaction proceeds rapidly once over the centrifugal barrier, i.e., there is no re-crossing of the barrier, and that the product distribution is frozen at that point.

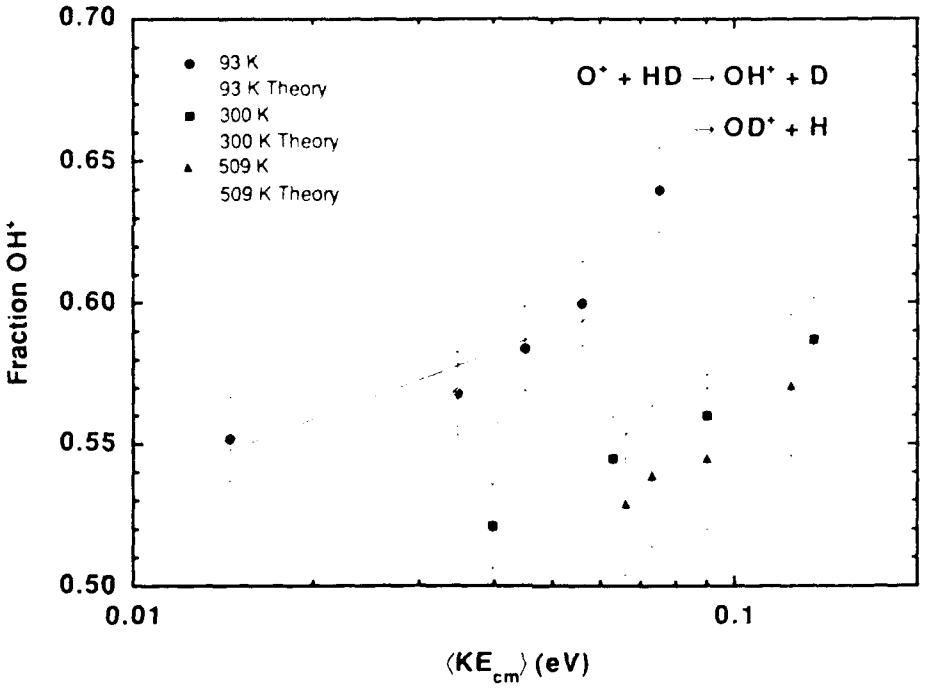

Figure 2. Branching fraction of OH^+ produced in the reaction of O^+ with HD as a function of $<KE_{cm}>$. Circles, squares, and triangles represent data taken at 93 K, 300 K, and 509 K, respectively. Theoretical curves[32] are given as solid, long dashed, and short dashed lines for 93 K, 300 K, and 509 K, respectively. (Reproduced with permission from ref. 38. Copyright 1992 American Institute of Physics)

The results of the theoretical calculations are shown in Figure 2 as a solid line, a large dashed line, and a small dashed line for temperatures of 93 K, 300 K, and 509 K, respectively. The theoretical results are integrated over Boltzmann distributions of rotations at the three temperatures and Boltzmann distributions of kinetic energies such that the average kinetic energy is given by $\langle KE_{cm} \rangle$. As stated earlier, drift tube measurements made in a helium buffer are adequately represented by Boltzmann distributions.[8-11] The low temperature data and theory are in very good agreement except at the highest kinetic energy. The branching fractions measured at higher temperature are smaller than the values predicted by theory by about 2 percentage points. This indicates that the theory slightly underestimates the rotational and kinetic energy dependences observed. The trends with energy, however, are reproduced very well.

The observed kinetic and rotational energy dependences may be understood in terms of simple physical ideas. The preference for OH^+ results from the fact that the center-of-mass (nearer to D than H) and the center of polarizability (the center of the HD bond) are different. This difference creates a torque on the HD molecule that tends to orient the H side of the molecule toward the O^+. The decreasing fraction of OH^+ formed in the reaction with increasing temperature at a given $\langle KE_{cm} \rangle$, i.e., the rotational energy dependence, arises from rotational averaging of the anisotropic potential as the HD rotates faster. As expected from this argument, the largest enhancement for OH^+ production should occur for low rotational quantum numbers. In fact, the theory of Dateo and Clary predicts the largest effect for $J = 0$ and smaller effects for large J (see Figure 5 in Dateo and Clary[32]). The increase in the fraction of OH^+ at higher kinetic energies may be understood as follows. At higher kinetic energies, the average impact parameter that leads to reaction is smaller. This constrains the centrifugal barrier to smaller radii where the anisotropy of the potential is larger, resulting in more alignment.

This reaction has also been studied by Burley et al.[33] in a guided ion beam mass spectrometer and more recently by Sunderlin and Armentrout in a modified version of the same apparatus with a variable temperature reaction cell.[34] The trends observed with ion kinetic energy and neutral gas temperature were the same as those observed in the present study. However, the magnitude of the temperature dependence at a given ion kinetic energy was smaller in value than that reported in this work. The difference in these observations arises from different ion velocity distributions in the two experiments. As mentioned above, the ion velocity distributions in our experiment are Maxwellian while those in the beam instrument are not. Support for this explanation comes from the theoretical predictions for the two experiments which incorporate the appropriate velocity distributions into the calculations and are in good agreement with the data.[34] As observed, the temperature dependence at a given ion kinetic energy is predicted to be smaller in the beam apparatus compared with that in the variable temperature drift tube.

The agreement between the predicted rotational energy dependence, the beam data, and the data obtained using our apparatus further validates the derivation of internal energy dependences from the observation of a temperature dependence of a kinetic parameter at a given $\langle KE_{cm} \rangle$. This is the first time that we have been able to compare data of this sort to other experimental or theoretical data.

c) The Reaction of O^- with H_2, D_2 and HD. The reaction of O^- with H_2 (and HD and D_2) proceeds by two channels, atom abstraction and associative detachment.

$$O^- + H_2 \rightarrow OH^- + H \qquad (8)$$
$$\rightarrow H_2O + e.$$

Our results for the reactions of O^- with H_2 and D_2 have been published elsewhere along with measurements on the effects of hydration of the O^- reactant on the reaction.[35] Figure 3 shows the rate constants for the reactions of O^- with H_2 and D_2 at three temperatures and with HD at 300 K. The rate constants are large and decrease slightly with increasing $\langle KE_{cm} \rangle$ or temperature. At a given $\langle KE_{cm} \rangle$, no temperature dependence of the rate constant is observed in the reactions of H_2 and D_2 over the range 176 K to 490 K, indicating that the reaction is not sensitive to the rotational temperature of the reactant neutral in this range, as expected for efficient reactions. The rate constants for the isotopes of hydrogen are in the order $k(H_2)>k(HD)>k(D_2)$, i.e., the rate coefficient decreases as the mass of the hydrogen isotope increases. The differences in the rate constants can be totally accounted for by the differences in the collision rate constants, which are inversely related to the square root of the reduced mass of the ion-neutral system. All of the reactions proceed with the same efficiency, on the order of 50%.

We have also measured the branching fractions of the two product channels. Figure 4 plots the percentage of the H/D atom abstraction channel forming the ionic products OH^- or OD^- versus $\langle KE_{cm} \rangle$. At low energies, only a few percent of ionic product is formed. This percent increases rapidly with increasing energy or temperature. The atom abstraction channel is more efficient in the reaction with H_2 than in the reaction with D_2. The efficiency of this channel for the reaction with HD was found to be approximately the same as measured for the reaction with H_2. The fact that the branching fraction for reaction with HD is similar to that for H_2 may be a real effect or may arise from a small systematic error due to the fact that the HD experiments were performed over a year after the H_2 and D_2 experiments, which were conducted in the same week. No rotational energy dependence is observed for the branching fractions in either of the reactions with H_2 or D_2, within our experimental uncertainty.

In addition to the total branching fraction to form ionic products, the relative abundances of OD^- and OH^- in the reaction of O^- with HD is of interest. We found that OD^- is formed preferentially in this reaction. The branching ratio of OD^- to OH^- was found to be 1.5:1, approximately independent of $\langle KE_{cm} \rangle$ over the entire energy range explored, 0.038 to 0.11 eV. This preference for formation of OD^- seemed surprising at first considering that OH^- is formed more frequently than is OD^- in the reactions with only one isotope. The preference for OD^- would be consistent with the fact that OD^- formation is about 0.04 eV more exothermic than OH^- production. However, this is inconsistent with preliminary results that indicate that at low temperature the preference for OD^- production is less. If thermodynamics controlled the branching, a larger, not smaller, preference for OD^- would be expected at low temperature. As will be shown below, the preference for OD^- can be readily explained.

The room temperature reactions of O^- with H_2 and D_2 were studied in a drift tube at the NOAA laboratories by McFarland et al.,[36] and our results are in very good agreement with theirs. McFarland et al. postulated a simple mechanism to explain their results. This mechanism also explains the HD data. They postulated a direct mechanism that proceeds in two steps. The first step is atom abstraction,

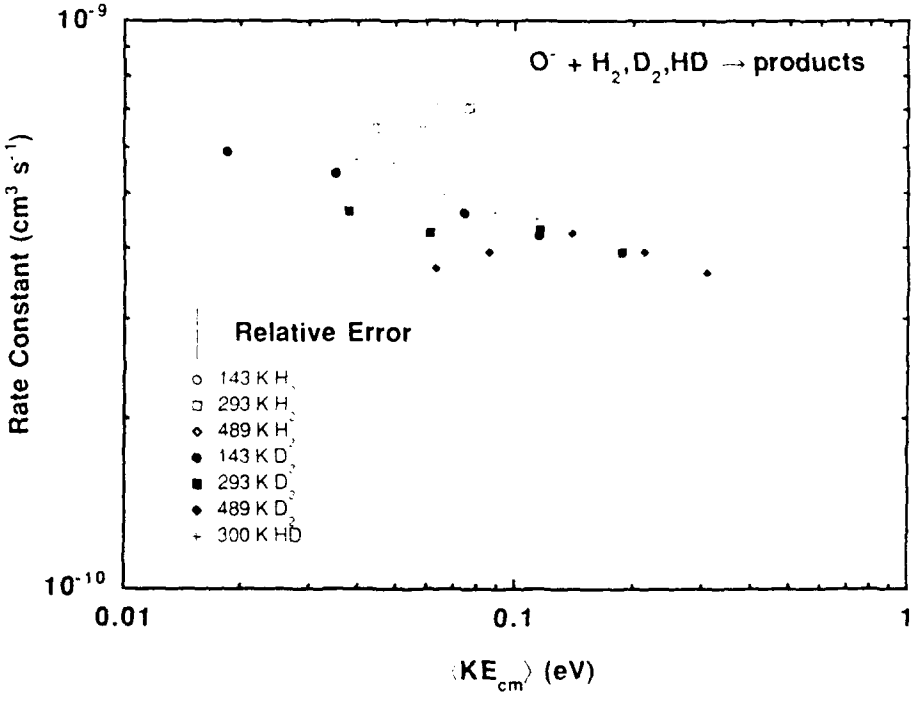

Figure 3. Rate constants for the reactions of O^- with H_2, D_2, and HD as a function of $\langle KE_{cm} \rangle$. Data for H_2 are represented by open circles, squares, and diamonds for temperatures of 143 K, 293 K, and 489 K, respectively. Data for D_2 are represented by solid circles, squares, and diamonds for temperatures of 143 K, 293 K, and 489 K, respectively. Data for HD are represented by plusses.

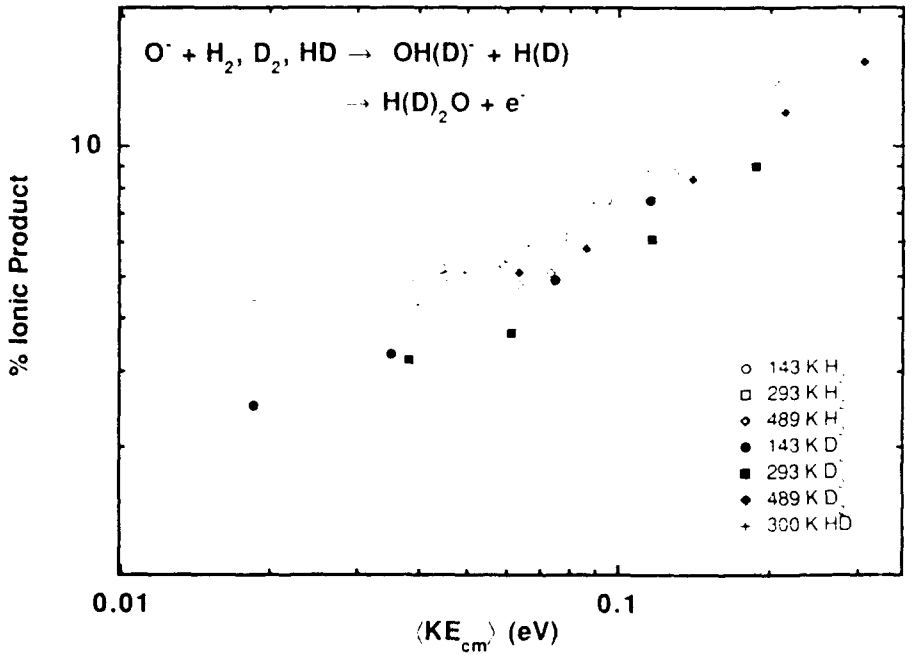

Figure 4. Branching percentages for the channel to produce the total ionic product (OH^- or OD^-) in the reactions of O^- with H_2, D_2, and HD as a function of $\langle KE_{cm} \rangle$. Data for H_2 are represented by open circles, squares, and diamonds for temperatures of 143 K, 293 K, and 489 K, respectively. Data for D_2 are represented by solid circles, squares, and diamonds for temperatures of 143 K, 293 K, and 489 K, respectively. Data for HD are represented by plusses.

$$O^- + H_2 \rightarrow \{OH^{-}\cdots H\}. \quad (9)$$

The H atom can then quickly separate from the OH^- leaving an ionic product,

$$\{OH^{-}\cdots H\} \rightarrow OH^- + H \quad (10)$$

or in the lifetime of the collision the OH^- can associatively detach,

$$\{OH^{-}\cdots H\} \rightarrow H_2O + e^-. \quad (11)$$

This simple mechanism seems to explain all of the features of the data. The associative detachment reaction (9 and 11) is known from separate experiments to be efficient.[1] This efficiency explains the predominance of this channel at low energy. As the energy is raised, the time that the OH^- and H spend near each other decreases, and the contribution by the OH^- channel increases. The overall reaction is relatively efficient, and rotational energy should have little influence. The relative branching fractions for the H_2 and D_2 reactions are explained by the ease with which the H or D atom can escape the initially formed $\{OH^{-}\cdots H\}$ complex. D atoms move more slowly than H atoms and will not escape from the complex as quickly as the H atom. As a result, the complex containing a D atom will have more time to pass through the critical configuration(s) for associative detachment. Therefore, one expects more associative detachment and thus less ionic product in the D_2 reaction compared with the H_2 reaction.

This prediction is borne out in the data. In the reaction with HD, two possible complexes may be formed initially. Either the D atom is transferred or the H atom is transferred. When the H atom is transferred to the O^-, a D atom is left behind. This complex, $\{OH^{-}\cdots D\}$ will result in more associative detachment than the other complex for the reasons discussed above, and less OH^- will be formed. Assuming that the two complexes are formed with equal probability, one predicts that OD^- will be formed more efficiently than OH^-, again in agreement with the observation. A rotational energy dependence similar to that observed in the reaction of O^+ with HD may occur in the atom abstraction step. However, such a dependence favors formation of OH^- over OD^-, a preference which is not observed. Therefore, any rotational energy dependence in the atom abstraction step is overwhelmed by the preference for formation of OD^- in the second step. We plan to examine the reaction for a small rotational energy dependence in this branching ratio in the future. In summary, the mechanism for this reaction, postulated almost twenty years ago, continues to explain all of the very detailed data observed for the isotopes of hydrogen.

d) The Reaction of O^- with CH_2D_2. The reaction of O^- with CH_4 produces OH^- with a rate constant on the order of 10^{-10} cm^3 s^{-1}.[3,4] At low energies the rate constant shows small negative dependences on both temperature and energy. Above approximately 0.1 eV the rate constant increases with increasing energy. In order to learn more about the mechanism of this reaction, we have begun a study involving isotopically labeled CH_4. Preliminary results (final results were not obtained in time to be included in this volume) indicate that substituting D for H decreases the rate constant substantially. For CD_4, the rate constant is on the order of a factor of ten lower than that for CH_4.

We have studied the branching fraction for the reaction of O^- with CH_2D_2, which produces both OH^- and OD^-. The results are shown in Figure 5. Plotted is the percent of the OH^- product formed as a function of $\langle KE_{cm} \rangle$. At low energies and temperatures, 90% of the total product is OH^-. This can be compared with the statistical (by number of H's or D's) prediction of 50%. Increasing temperature or energy decreases the OH^- branching fraction. Even at $\langle KE_{cm} \rangle$ approaching 0.5 eV the OH^- product still dominates, constituting 60% of the products formed. The data also indicate that the branching fraction does not depend on the rotational energy or low frequency vibrations of the CH_2D_2.

The strong preference for formation of OH^- over OD^- and the decrease in the rate constant with deuterium substitution can be explained by a barrier in the potential energy surface. Figure 6 shows a calculated ab initio potential energy curve for the reaction coordinate of the reaction of O^- with CH_4. The calculations were carried out at the HF/6-31++G(d,p) level of theory.[37] This curve represents the minimum energy pathway along the ground $\{^2A_1\}$ surface for the reaction of O^- with CH_4 leading to OH^- and CH_3 products. A second reaction pathway along the first excited $\{^2E\}$ surface leads to OH and CH_3^- products. This latter reaction pathway was not energetically accessible for the range of collision energies in our studies. Figure 6 indicates that a small barrier to the ground state reaction is found with a classical barrier height of approximately 0.02 eV, essentially at the zero of energy within the uncertainty of the calculations. The classical reaction pathway illustrated in Figure 6 must be modified to account for quantum effects of rotation and vibration. The quantum corrected barrier will be slightly smaller than the classical barrier. Correlated energy calculations along this reaction pathway, which are currently in progress, should reduce the uncertainty in locating the barrier height to less than 0.08 eV.

In Table 1, we list the thermochemistry for reactions of O^- with isotopically substituted CH_4. We find that the reaction exothermicity is greatest for O^- with CH_4 and least for O^- with CD_4. The strong preference observed in the branching fraction and the decrease observed in the rate constant for abstraction with D substitution can be explained by zero point energy effects. The overall exothermicity[37] for the reaction of O^- with CH_4 is 0.258 eV, while that for the reaction of O^- with CD_4 is 0.205 eV, i.e., the reaction is 0.053 eV less exothermic for the perdeuterated form. Similar differences are found for the two channels in the reaction of O^- with CH_2D_2, since the bond strengths for the C-H and C-D in CH_2D_2 are similar to those in the pure isotopes. This exothermicity difference shows that the difference in zero point energies makes it slightly harder to break the C-D bond than the C-H bond. This will be reflected in the quantum corrected barrier height. For reactions involving D abstraction, the barrier will be slightly higher than for reactions involving H abstraction. The increased barrier height will in turn slow the rate of D abstraction compared to the rate of H abstraction. This is reflected in the data in both the branching fraction and the rate constants. We note that Figure 6 indicates a broad barrier along the minimum energy reaction coordinate. This suggests that quantum tunneling effects are negligible for this system.

Conclusions

We have presented data on four reactions in which isotopic labeling is used to help determine the reaction mechanism. In the reaction of O^- with N_2O, the labeling of the

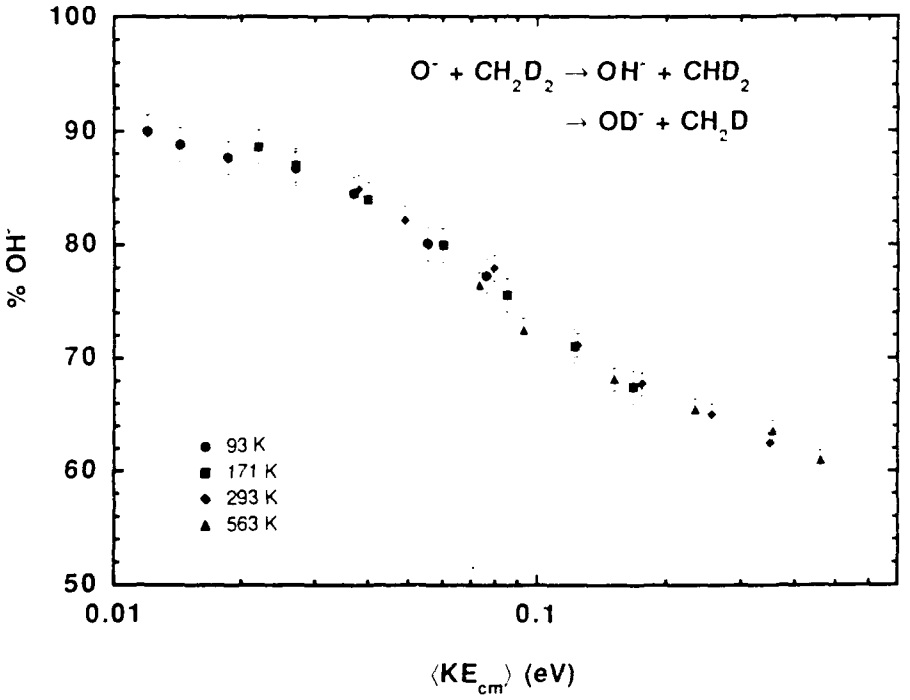

Figure 5. Branching percentage of OH^- produced in the reaction of O^- with CH_2D_2 as a function of $\langle KE_{cm} \rangle$. Circles, squares, diamonds, and triangles represent data for temperatures of 93 K, 171 K, 293 K, and 563 K, respectively.

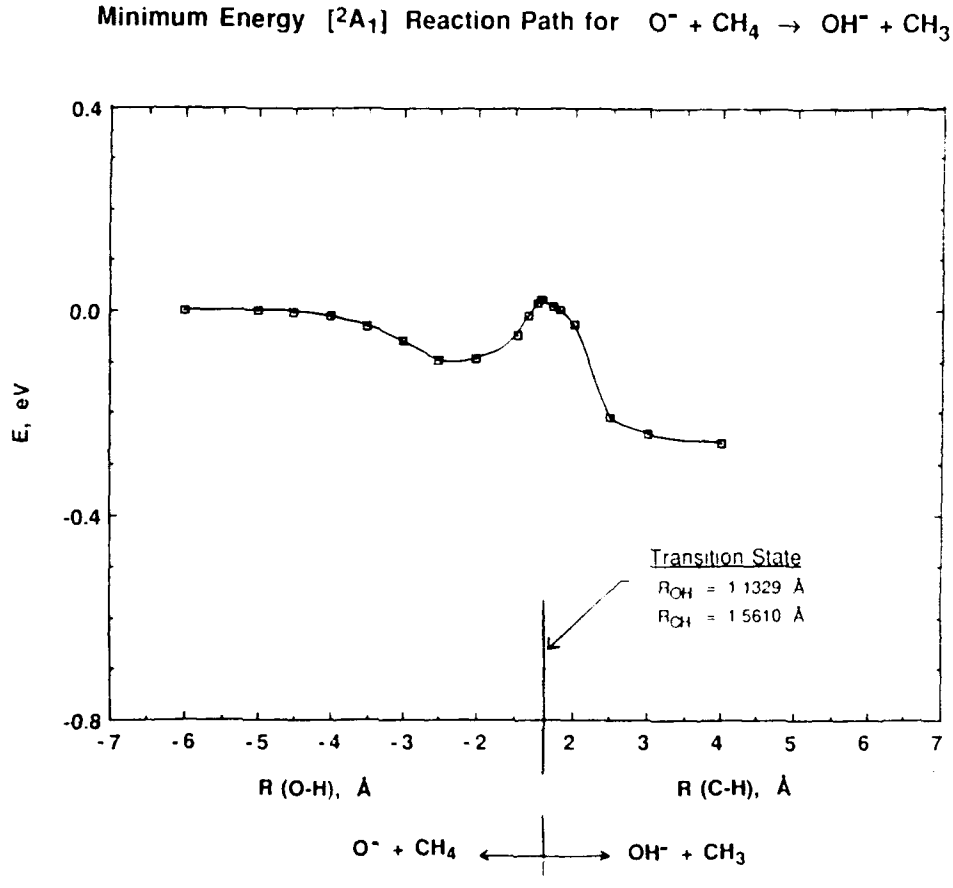

Figure 6. Reaction path diagram for the reaction of O^- with CH_4.

Table 1. Thermochemistry of the Reactions of O^- with CH_4, CD_4, and CD_2H_2.[37]

Reaction	$-\Delta H_R$ (eV)		
	96 K	298 K	500 K
$O^- + CH_4 \rightarrow OH^- + CH_3$	0.284	0.258	0.232
$O^- + CD_4 \rightarrow OD^- + CD_3$	0.232	0.205	0.188
$O^- + CD_2H_2 \rightarrow OH^- + CD_2H$	0.263	0.235	0.212
$O^- + CD_2H_2 \rightarrow OD^- + CDH_2$	0.257	0.231	0.210

reactants helped to determine the relative preference for attack of the O^- at the central and terminal nitrogens. The study did not yield unambiguous results but did indicate that a large fraction of the reactive encounters occurs by attack at the central nitrogen, in contrast with studies involving other anions reacting with N_2O.[30,31]

The reaction of O^+ with HD shows a large preference for OH^+ production at low temperatures and moderate energies. A model based on entrance channel effects seems to explain the data.[32] The branching fraction is determined by such effects as the speed of the HD rotations, the torque arising from the different positions of the center-of-mass and center-of-polarizability, and the location of the centrifugal barrier. The confirmation of a rotational energy dependence in this reaction helps to validate the technique in which variable temperature drift tube studies are used to derive information on internal energy effects in ion-molecule reactions.

The reactions of O^- with H_2, D_2, and HD are explained by a two-step mechanism. The rate constants vary with the mass of the hydrogen molecule, as predicted by the mass-dependent collision rate, while the efficiency of the reaction remains constant. Isotopic effects in the branching fractions are most easily explained by the relative velocity of the departing H or D atom. The slower D atom allows more time for the complex to assume the critical configuration(s) necessary for associative detachment.

Finally, in the reaction of O^- with CH_4 and its deuterated analogs, zero point energy effects play a major role in both the observed rate constant and product branching fractions. The greater exothermicity of the reactions involving H abstraction leads to the rate constant for CH_4 being larger than that for CD_4 and also leads to a branching fraction for the reaction with CH_2D_2 which greatly favors OH^- production.

The mechanisms for all four of these reactions have little in common. Taken together, these four studies show the utility of using isotopically labeled reactants to elucidate a variety of reaction mechanisms. One has only to look at other chapters in this volume to see more such examples.

Acknowledgements

This research was sponsored in part by the United States Air Force under Contract No. F19628-86-C0224 and F49620-89-C-0019. The United States Government is authorized to reproduce and distribute reprints for governmental purposes notwithstanding any copyright notation herein.

Literature Cited

1. Ikezoe, Y.; Matsuoka, S.; Takebe, M.; Viggiano, A. A. *Gas Phase Ion-Molecule Reaction Rate Constants Through 1986.*; Maruzen Company, Ltd.: Tokyo, 1987.
2. Viggiano, A. A.; Morris, R. A.; Dale, F.; Paulson, J. F.; Giles, K.; Smith, D.; Su, T. *J. Chem. Phys.* **1990**, *93*, 1149.
3. Viggiano, A. A.; Morris, R. A.; Paulson, J. F. *J. Chem. Phys.* **1988**, *89*, 4848.
4. Viggiano, A. A.; Morris, R. A.; Paulson, J. F. *J. Chem. Phys.* **1989**, *90*, 6811.
5. Viggiano, A. A.; Van Doren, J. M.; Morris, R. A.; Paulson, J. F. *J. Chem. Phys.* **1990**, *93*, 4761.
6. Smith, D.; Adams, N. G. *Adv. At. Molec. Phys.* **1988**, *24*, 1.
7. Wannier, G. H. *Bell. Syst. Tech. J.* **1953**, *32*, 170.
8. Viehland, L. A.; Robson, R. E. *Int. J. Mass Spectrom. Ion Processes* **1989**, *90*, 167.
9. Viehland, L. A.; Viggiano, A. A.; Mason, E. A. *J. Chem. Phys.* **1991**, submitted.
10. Dressler, R. A.; Beijers, J. P. M.; Meyer, H.; Penn, S. M.; Bierbaum, V. M.; Leone, S. R. *J. Chem. Phys.* **1988**, *89*, 4707.
11. Dressler, R. A.; Meyer, H.; Langford, A. O.; Bierbaum, V. M.; Leone, S. R. *J. Chem. Phys.* **1987**, *87*, 5578.
12. Viggiano, A. A.; Morris, R. A.; Paulson, J. F. *J. Phys. Chem.* **1990**, *94*, 3286.
13. Su, T.; Morris, R. A.; Viggiano, A. A.; Paulson, J. F. *J. Phys. Chem.* **1990**, *94*, 8426.
14. Travers, M. J.; Cowles, D. C.; Ellison, G. B. *Chem. Phys. Lett.* **1989**, *164*, 449.
15. Albritton, D. L.; Dotan, I.; Lindinger, W.; McFarland, M. *J. Chem. Phys.* **1977**, *66*, 410.
16. Albritton, D. L. In *Kinetics of Ion-Molecule Reactions*; Ausloos, P., Ed.; Plenum Press: New York, 1979.
17. Grabowski, J. J.; DePuy, C. H.; Bierbaum, V. M. *J. Am. Chem. Soc.* **1983**, *105*, 2565.
18. Lias, S. G.; Bartmess, J. E.; Liebman, J. F.; Holmes, J. L.; Levin, R. D.; Mallard, W. G. *J. Phys. Chem. Ref. Data* **1988**, *17, Supplement 1*, 1.
19. Morris, R. A.; Viggiano, A. A.; Paulson, J. F. *J. Chem. Phys.* **1990**, *92*, 3448.
20. Van Doren, J. M.; Barlow, S. E.; DePuy, C. H.; Bierbaum, V. M. *J. Am. Chem. Soc.* **1987**, *109*, 4412.
21. Barlow, S. E.; Bierbaum, V. M. *J. Chem. Phys.* **1990**, *92*, 3442.
22. Paulson, J. F. *Adv. Chem. Ser.* **1966**, *58*, 28.
23. Posey, L. A.; Johnson, M. A. *J. Chem. Phys.* **1988**, *88*, 5383.
24. Hacaloglu, J.; Suzer, S.; Andrews, L. *J. Phys. Chem.* **1990**, *94*, 1759.
25. Jacox, M. E. *J. Chem. Phys.* **1990**, *93*, 7622.
26. Magnera, T. F.; Kebarle, P. In *Ionic Proc. Gas Phase*; Almoster Ferreira, M.A., Eds.; D. Reidel Publishing: Boston, 1984.
27. Troe, J. *Int. J. Mass Spectrom. Ion Processes* **1987**, *80*, 17.
28. Troe, J. In *Advances in Chemical Physics. State-selected and State-to-state Ion-molecule Reaction Dynamics: Theoretical Aspects, Part 2*; Baer, M., Ng, C. Y., Eds.; John Wiley: New York, in press.
29. Deakyne, C. A., private communication, 1989.

30. Kass, S. R.; Filley, J.; Van Doren, J. M.; DePuy, C. H. *J. Am. Chem. Soc.* **1986**, *108*, 2849.
31. Bierbaum, V. M.; DePuy, C. H.; Shapiro, R. H. *J. Am. Chem. Soc.* **1977**, *99*, 5800.
32. Dateo, C. E.; Clary, D. C. *J. Chem. Soc. Faraday Trans. II* **1989**, *85*, 1685.
33. Burley, J. D.; Erwin, K. M.; Armentrout, P. B. *Int. J. Mass Spectrom. Ion Processes* **1987**, *80*, 153.
34. Sunderlin, L. S.; Armentrout, P. B. *Chem. Phys. Lett.* **1990**, *167*, 188.
35. Viggiano, A. A.; Morris, R. A.; Deakyne, C. A.; Dale, F.; Paulson, J. F. *J. Phys. Chem.* **1991**, *95*, 3644.
36. McFarland, M.; Albritton, D. L.; Fehsenfeld, F. C.; Ferguson, E. E.; Schmeltekopf, A. L. *J. Chem. Phys.* **1973**, *59*, 6629.
37. Frisch, M. J.; Head-Gordon, M.; Trucks, G. W.; Foresman, J. B.; Schlegel, H. B.; Raghavachari, K.; Robb, M. A.; Binkley, J. S.; Gonzalez, C.; DeFrees, D. J.; Fox, D. J.; Whiteside, R. A.; Seeger, R.; Melius, C. F.; Baker, J.; Martin, R. L.; Kahn, L. R.; Stewart, J. J. P.; Topiol, S.; Pople, J. A. *Gaussian 90* (Carnegie - Mellon Quantum Chemistry Publishing Unit, Pittsburgh, PA, 1990).
38. Viggiano, A. A.; Van Doren, J. M.; Morris, Williamson, J.S., Mundis, P. L.; R. A.; Paulson, J. F. *J. Chem. Phys.* **in press.**

RECEIVED October 16, 1991
Reprinted from ACS Symposium Series No. 502
Isotope Effects in Gas-Phase Chemistry
Jack A. Kaye, Editor